HIGHLY SENSITIVE LASER SPECTROSCOPY OF ATMOSPHERIC GASES

L.N. Sinitsa

Institute of Atmospheric Optics,
Siberian Branch of the Russian Academy of Sciences, Tomsk
Received September 30, 1994

The investigations performed at the Institute of Atmospheric Optics to design a high−sensitivity laser spectrometers as well as the results obtained with them are reviewed in this paper. The laser spectrometers based on spectrophotometric, opto−acoustic, and intracavity methods allow weak absorption spectra within range from 800 to 16000 cm^{-1} to be studied successfully with 10^{-2} to 10^{-4} cm^{-1} resolution. Thousands of new absorption lines and tens of earlier unknown vibrational−rotational bands of atmospheric and polluting gases were detected using the spectrometers. The analysis of the spectra allowed us to determine the energy structure and spectroscopic constants of high vibrational states of molecules as well as the coefficients of the shifts caused by buffer gases pressure.

At present the main tendencies in the development of up−to−date experimental methods of molecular spectroscopy of the atmospheric gases are connected with the improvement in spectral resolution and absorption sensitivity of the instrumentation as well as with the use of new spectral regions and wider application of the research achievements. The high monochromaticity of laser emission used in facilities for atmospheric studies, in combination with the selectivity of atmospheric absorption spectra in the optical range, and large dynamic range in the variations of absorption coefficients (from 10^{-4} cm^{-1} at the centers of strong lines down to 10^{-8} cm^{-1} for weak lines in atmospheric transmission windows) require qualitatively new spectroscopic information for solving many practical problems of atmospheric optics.[1]

For solving these problems a program of development of high resolution laser spectrometers was formulated at the Institute of Atmospheric Optics (IAO) by V.E. Zuev, and first laser spectrometer with a narrow−band tunable ruby laser and a multipass absorption cell was constructed at the IAO in 1970.[2]

During the past twenty five years, highly sensitive methods of the absorption laser spectroscopy have been developed in order to satisfy increasing needs of the atmospheric optics. These methods had spectral resolutions of 10^{-2} to 10^{-4} cm^{-1} and sensitivities of 10^{-7} to 10^{-9} cm^{-1} which allowed one to investigate weak lines in absorption spectra of the atmospheric and contaminating gases.

This paper presents the investigations of laser spectrometers and quantitative data on the absorption spectra obtained with them at the Institute of Atmospheric Optics.

1. LASER SPECTROMETERS

Depending on the technique used for recording the amount of energy absorbed by a substance from a laser beam the methods are divided into three groups, viz., spectrophotometric, opto−acoustic, and intracavity absorption methods.

1.1 Laser spectrophotometry

The spectrophotometric method of the absorption coefficient measurements is based on comparison of the radiation incident on and passed through an absorbing medium. The value k(v) is calculated in this case using the Bouguer−Lambert−Beer law.

Block−diagram of a high−resolution Neodymium−glass laser spectrophotometer is depicted in Fig. 1. The laser spectrophotometer was developed on the basis of a running−wave ring−cavity laser with continuous frequency tuning during the generation pulse.[3] Instantaneous width of the laser emission line was extremely narrow (less than 2 MHz) and tuned within 0.7 cm^{-1} during a single pulse. The total spectral range of the laser emission from 9240 to 9500 cm^{-1} was covered by pulse to pulse tuning when rotating a dispersion prism installed inside the laser cavity. The position of the laser emission line was determined using a grating spectrometer accurate to 0.08 cm^{-1}. Precise frequency measurements (accurate to 0.001 cm^{-1}) were carried out using a thermostated and evacuated Fabry−Perot etalon with the spacing ring 103.5 mm thick.

Since the lasing process strongly depends on the absorption of radiation by air inside the cavity, the laser may operate in two modes, i.e., as a narrow−band intracavity spectrometer or as a laser spectrophotometer.

When the laser operates in the first mode its cavity involves two cells 70 cm long which are filled with a gas to be studied. The selective losses inside the laser cavity produce a perturbation affecting on the laser in a stationary quasicontinuous regime of generation. Selective absorption of radiation is recorded in the narrow−band intracavity laser (ICL) spectroscopy technique by detecting a gap in the time behavior of the intensity of a single mode laser emission in contrast to the broad−band ICL spectroscopy method where the gap is formed in the spectrum of a multimode laser emission.
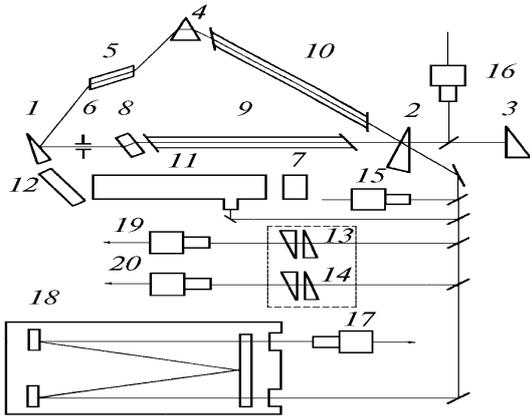
FIG. 1. Block—diagram of a high—resolution laser spectrophotometer with Nd:glass ring—cavity laser. 1, 2, and 3 are the cavity mirrors; 4 is the prism; 5 is the active laser media; 6 is the diaphragm; 7 is the optical multichannel analyzer; 8 is the plane—parallel plate; 9 and 10 are the cells; 11 and 12 are the polychromator; 13 and 14 are the Fabry—Perot interferometer; 15, 16, 17, 19, and 20 are the photodetectors; and, 18 is the multipass cells.

In the second version the intracavity absorption cells are evacuated that makes it possible to obtain a smooth laser pulse even if there are strong lines of atmospheric absorption in the range of the laser frequency tuning. Laser radiation is directed into a 3—m long multipass absorption cell of the White type adjusted for obtaining a 280—m long path. Intensity of the light beam incident on the absorption cell was about 100 times lower than that of the output laser beam and, as the simplest estimations show, there were no nonlinear absorption effects and gas heating under these experimental conditions. The width of the laser emission line in this case was about two orders of magnitude less than that of Doppler contours of the absorption lines investigated that enabled us to neglect the influence of the instrumental function of the spectrometer on the final results of measurements.

High sensitivity of laser spectrophotometers is provided by the use of multipass gas absorption cells. A three mirrors scheme suggested by White[4] has been used for more than 40 years to increase the sensitivity of different spectrometers. At present multipass systems of new generation, i.e., the so—called matrix multireflection systems[5] allowed us to achieve in the cells of 110 m length the path lengths up to 15 km. Parameters of the spectrophotometer are presented in Ref. 6 and in Table I.

TABLE I. Parameters of laser spectrophotometers.

Laser	Spectral range, cm^{-1}	Spectral resolution, cm^{-1}	Absorption sensitivity, cm^{-1}	Path length, m
Ruby	14395—14405	10^{-3}	10^{-8}	60—4000
Dye	16500—16900	$7 \cdot 10^{-4}$	$5 \cdot 10^{-9}$	110—10000
Alexandrite	12500—14000	$5 \cdot 10^{-3}$	10^{-8}	60—4000
Nd:glass	9240—9520	$7 \cdot 10^{-4}$	10^{-7}	12—228
Diode	2000—6000	10^{-3}	10^{-7}	12—228

1.2. Opto—acoustic spectroscopy

The opto—acoustic (OA) method is a calorimeter technique based on measurements of radiation power absorbed by a substance under study. When a laser radiation pulse passes through a cell with a gas under study the gas heats due to absorption (if it occurs) of the radiation. This heat exchange, in a closed volume of the cell, produces the pressure pulse, which, when recorded with a sensitive pressure sensor (e.g., by a microphone), bears the information about the absorption properties of the gas.

In the case of weak absorption ($k(\nu) L_\alpha \ll 1$) which normally occurs in the high—frequency spectral range, the amplitude of the pressure oscillations A_p inside the cell is proportional, at the pulse excitation, to the energy of incident radiation and to the absorption coefficient, i.e.,

$$A_p = \alpha_p \cdot k(\nu) E .$$

In the case of a modulated cw laser radiation, the pressure pulse amplitude is proportional to the power W of laser radiation

$$A_{cw} = \alpha_{cw} \cdot k(\nu) W .$$

Thus the opto—acoustic spectrometer signal is linearly related to the absorption coefficient of a medium in contrast to that of the spectrophotometer signal which measures the transmission of a medium.

The detection sensitivity of the opto—acoustic spectrometers can be improved by 10 to 100 times by placing OA detector in the laser cavity. The OA spectrometer with two detectors inside the cavity of a dye laser had the threshold sensitivity of $< 10^{-9}$ cm^{-1} for the power of 0.1 W and was effectively used for investigation into the HDO spectrum and line shifts of H_2O in 0.6 μm region.[7] Parameters of OA spectrometers are presented in Ref. 6 and Table II.

TABLE II. Parameters of the laser OA spectrometers.

Laser	Spectral range, μm	Absorption sensitivity, cm^{-1}	Spectral resolution, cm^{-1}	Error of K measurements (%)
Tunable dye laser (R6G)	0.58—0.63	$3 \cdot 10^{-8}$	10^{-4}	10—12
Tunable ruby and Nd:glass lasers	˜ 0.69 ˜ 1.06	10^{-8}	10^{-2}	12—15
Pulsed CO_2 laser tuned from line to line	˜ 10.6	10^{-7}	10^{-2}	15—20
Intracavity OAS with tunable cw dye laser (R6G)	0.6—9.4	10^{-9}	10^{-3}	˜ 10

1.3. Intracavity laser spectroscopy

The method of broad–band ICL spectroscopy proposed in 1970 (Ref. 8) consists of quenching the laser emission at the frequencies of absorption lines of species placed in a broad–band laser cavity, the generation band width of such a laser $\Delta \nu_g$ being much greater than the half–width of spectral line studied. In this case the laser emission spectrum has sharp gaps at the frequencies of absorption lines, which can be recorded with an ordinary spectroscopic instrumentation. In the intracavity laser spectroscopy a laser itself is a nonlinear detector of weak absorption.

In case when one can neglect the spectral behavior of the gain coefficient $\kappa(\nu)$ ($\kappa(\nu) = \kappa_0 = $ const) and the contribution from spontaneous emission at the stage of quasicontinuous generation (also for the case of a square–shaped pumping pulse and stable mode structure) the ICL spectrum in the vicinity of an absorption line normalized by its maximum can be described as follows[9]:

$$J(\nu, t) = U(\nu, t)/U_m(t) = J(\nu, t_0)\cdot\exp[-k(\nu) L_{eff}] ,$$
$$L_{eff} = c\, t\, L_a/L_c , \qquad (1)$$

where $J(\nu, t_0)$ represents the normalized spectrum formed at the starting moment of generation t_0, $U(\nu, t)$ is the radiant exitance at the frequency ν at time t, $U_m(t)$ is the value of $U(\nu, t)$ at frequencies off the absorption line, L_a is the length of the absorbing layer, and L_c is the length of the laser cavity. If one neglects the pregeneration stage then it is possible to assume that $U(\nu, t_0) = 1$ and hence the depth of a gap in the ICL spectrum is determined by the Bouguer law. That means that the laser, in this sense, imitates a multipass absorption cell, but with much greater effective length L_{eff} of the absorbing layer than in a simple multipass cell where it is limited by radiation losses on mirrors. In this case L_{eff} is proportional to duration t of continuous generation in the region of an absorption line studied (see Fig. 2), $L_{eff} = ct\mu_a$, where c is the speed of light, and μ_a is the filling factor for a resonator filled with a substance under study.

The threshold sensitivity of the ICL spectroscopy technique k_{min} (i.e., the value of the absorption coefficient corresponding to a preset detectable depth of ICL spectrum gap $D_a = J(\nu_0, t)$) can be written as

$$k_{min} = (\ln D_a - \ln D_0)/L_{eff} , \qquad (2)$$

where $D_0 = J(\nu_0, t_0)$. At 1 ms duration of the quasicontinuous generation and $\mu_a = 1$, the effective length L_{eff} can reach $3\cdot10^5$ m which enables one to detect absorption lines with the absorption coefficient $k_{min} = 3\cdot10^{-9}$ cm^{-1} if $D_0 = 0.9$.

The intracavity laser spectrum reproduces the response of the emission spectrum on the optical losses inside the cavity caused by absorbing properties of a substance placed into it, but this response does not simply reproduce actual absorption spectrum. Expression (1) makes a basis for quantitative measurements since it describes the processes taking place in ICL spectrometer and directly relates the depth of a gap in the emission spectrum to the absorption coefficient and duration of generation.
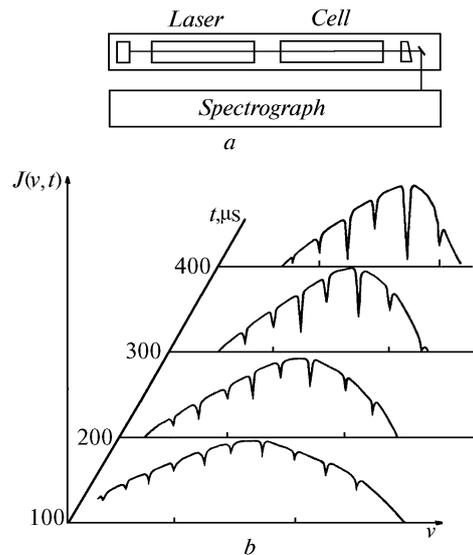

FIG. 2. Block–diagram of an ICL spectrometer (a). Emission spectrum of a broad–band laser with the selective intracavity losses at different time moments (b).

At present there are a number of ICL spectrometers constructed at the Institute based on color center lasers, ruby, Neodymium–glass, and dye lasers pumped by flash lamps or by an external lasers, covering, on the whole, the spectral range wider then 3000 cm^{-1} in the visible and photographic IR regions. Parameters of the spectrometers are given in Table III.

TABLE III. Parameters of ICL spectrometers.

Laser	Spectral range, cm^{-1}	Spectral resolution, cm^{-1}	Absorption sensitivity, cm^{-1}	Spectral range per pulse, cm^{-1}
Broad–band spectrometers				
Dye	16500–16900	0.05	10^{-7}	20–100
Ruby	14395–14405	0.02	10^{-8}	0.5–3
Nd:glass	9100–9520	0.02	10^{-8}	20–100
Nd:glass	7350–7400	0.05	10^{-7}	5–10
F_2^+: LiF	10400–11000	0.05	10^{-7}	50–100
F_2^-: LiF	8000–9000	0.05	10^{-8}	50–100
K Zn F^3: Cr^{3+}	12207–12272	0.05	$8\cdot10^{-8}$	5–20
Single–mode spectrometer				
Nd:glass	9200–9500	0.005	10^{-7}	1–2

The method of ICL spectrometry can be applied to solution of both traditional molecular spectroscopy and atmospheric optics problems, and of many other, qualitatively new problems. This is caused by a number of the technique's advantages: high sensitivity of the detection of super weak absorption (absorption factor 10^{-8} cm^{-1}), which corresponds to the use of 10 000–m absorption path in classical spectroscopy, high time resolution (1μs–1ms) that is necessary for investigation of fast processes, and wide spectral ranges in the visible and photographic infrared regions. Fast response enables one to cover range of 50 to 200 cm^{-1} per one pulse at high spectral resolution.

Comparison of the atmospheric absorption spectrum recorded in a solar spectrum and obtained using the intracavity spectrometer is presented in Fig. 3. It is evident from this figure that even in such a narrow portion of the spectrum there appear a lot of new weak lines.
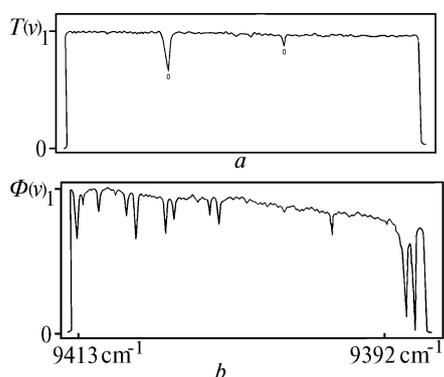

FIG. 3. Absorption spectrum of the atmosphere in the region 9392–9413 cm^{-1} (strong lines are the Fraunhofer lines) recorded using solar radiation (a) and the atmospheric absorption spectrum obtained with an ICL spectrometer[13] (b).

The spectrophotometric technique is used in measurements of absolute values of the spectral absorption coefficients. It allowed the measurements of the absorption spectra of different gases contaminating the atmosphere to be made with the spectral resolution 10^{-2} to 10^{-4} cm^{-1} within the emission ranges of different types of lasers including dye lasers, semiconductor lasers, solid state lasers, and so on.

Higher sensitivity at smaller size is provided by opto–acoustic and intracavity technique. The opto–acoustic method is simplest for performance in a device and very efficient in the IR region.

The ICL spectroscopy technique allows one to record a wide portion of a absorption spectrum of a gas during a short time interval, it is also convenient for studying excited states of molecules.

These methods complement each other and can be very efficient when used in combination.

2. INVESTIGATION OF HIGHLY EXCITED MOLECULAR STATES

High–sensitivity laser spectrometers allowed the recording of several thousands new atmospheric absorption lines to be performed in the spectral range above 8000 cm^{-1}. Some tens of earlier unknown vibrational–rotational bands of H_2O, CO_2, N_2O, CH_4, C_2H_2, NH_3, HBr, and H_2

molecules and their isotopomers have been also recorded with these devices.

For example, one can see in Fig. 4 the vibrational–rotational bands of the atmospheric and contaminating gases, the fine structure of which was studied using high–resolution ($7 \cdot 10^{-4}$ to $8 \cdot 10^{-2}$ cm^{-1}) spectrometers in the ranges of Nd:glass, F_2^+:LiF and F_2^-:LiF color center lasers emissions.[14] Some experiments demonstrating the efficiency and usefulness of the laser spectroscopy method are described below.
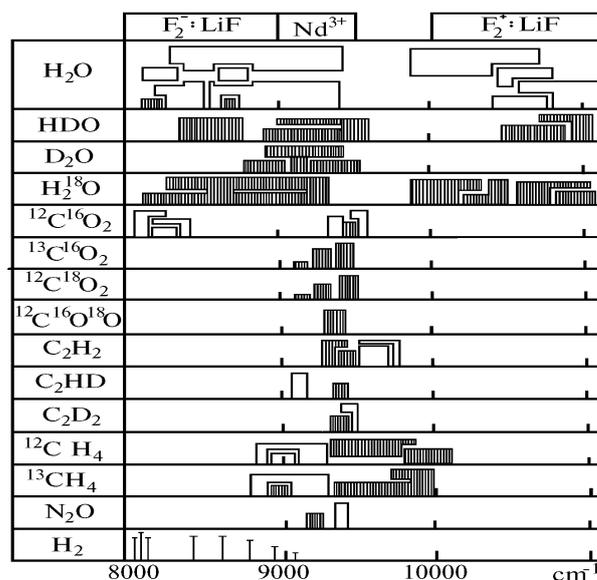

FIG. 4. Molecular absorption bands in the region 8000–11100 cm^{-1}, studied using laser spectrometers (dashed portions show newly recorded absorption bands).

2.1. Absorption spectra of linear molecules

In absorption spectra of linear molecules $^{12}C^{16}O_2$, $^{13}C^{12}O_2$, $^{12}C^{18}O_2$, $^{12}C^{16}O^{18}O$, N_2O, C_2H_2, C_2HD, and C_2D_2, some new vibrational–rotational bands with $\Delta V \geq 4$ were recorded, and the rotational structure of Q branches was resolved.[14–16] The Fermi–resonance 2003 triad was also investigated in different isotopes of the carbon dioxide. As a result of solving the inverse spectroscopic problem, the vibrational transitions were identified, and some spectroscopic constants of the molecules as well as the energies of vibrational–rotational levels were determined. Spectroscopic constants of the upper vibrational states of linear molecules are presented in Table IV.

Molecule H_2 does not possess any dipole moment, therefore, it is not active in the IR spectral range, and it has not any allowed absorption spectra in its ground electronic states. The molecular electric dipole moment can be induced by an external electric field. The induced absorption spectrum of hydrogen molecule was studied using the ICL spectrometers. A special high–pressure cell with capacitor plates inside it was constructed. The cell can be used at gas pressures up to 20 atm and at capacitor voltages up to 50 kV, providing the electric field strength as high as 120 000 V/cm (see Ref. 17).

TABLE IV. Spectroscopic constants of highly excited vibrational states of linear molecules (cm^{-1}).

Gas	State			E_v	B_v	$D_v \, 10^7$
$^{12}C^{16}O_2$	20032			9516.98(2)	0.38048(4)	1.4(7)
	20033			9388.97(1)	0.38238(5)	1.7(3)
	10031			8293.93(2)	0.38086(9)	1.4(3)
	10032			8192.54(2)	0.38156(7)	1.5(2)
	21132	c	o	1045.50(3)	0.38088(3)	1.1(7)
		d		10145.49(3)	0.38222(3)	0.6(9)
	11132	c	o	8803.27(2)	0.38187(8)	1.4(8)
		d		8803.28(2)	0.38276(8)	1.5(7)
$^{13}C^{16}O_2$	20031		o	9404.11(3)	0.38071(13)	1.4(9)
	20032		o	9302.12(1)	0.38122(6)	1.6(7)
$^{12}C^{18}O_2$	20031		*	9451.81(2)	0.33918(8)	1.5(9)
	20032		*	9307.20(2)	0.33842(9)	1.4(7)
	20033		*	9197.83(3)	0.33900(13)	1.9(9)
$^{12}C^{16}O^{18}O$	20032		*	9412.76(2)	0.35884(16)	1.2(8)
C_2H_2	2100^01^1	d	*	9366.61(3)	1.1619(3)	8.9(6)
		c			1.1566(3)	6.5(8)
	1200^03^1	d	*	9407.72(4)	1.1695(5)	2.8(10)
		c			1.1592(5)	3.6(15)
C_2D_2	2110^00^0			9444.52(1)	0.8287(1)	8.0(6)
	2110^01^1		*	9963.76(3)	0.8111(3)	8.0(6)
C_2HD	2010^00^0			9138.87(2)	0.9898(3)	9.0(5)
N_2O	40021			9294.93(2)	0.40637(6)	1.8(6)
	40022		*	9218.80(3)	0.4080(6)	2.0(2)

The values of 68% confidence intervals, expressed in the last significant digits, are given in brackets.
* — new vibrational–rotational states;
o — the bands observed previously in the spectrum of Venus atmospheric absorption only.

Energies of rotational levels of the vibrational state V = 2 were determined for the first time and spectroscopic parameters of the upper vibrational state of H_2 molecule were improved.[18]

2.2. Investigation of water vapor energy levels

A special approach is required for assignment and analysis of H_2O spectra in high–frequency region. The reasons for this are twofold. First, for weak bands it is difficult to find two or more lines sharing the same upper level. As a rule, we have a single line for energy level determination; other transitions to the same upper level are too weak to be recorded. Hence, there is no confirmation of assignments by the observation of combination differences. In this situation, one has to make effective the use of predicted calculations of line positions on the basis of preliminary fitting at every step of the assignment. It is obvious, that in order to make useful predictions, one needs for accurate estimates of vibrational, rotational, and resonance coupling constants of all upper states to allow for the resonance perturbations of line positions in the bands under considerations.

Second, those members of a resonance polyad which are not observable, but may perturb the observed levels, play the role of "dark" states. These states must be taken into account both in the preliminary calculations and in the final fitting of the spectroscopic constants for the assigned transitions. Information is thus required about all the upper vibrational states that may be involved.

So we need to develop a new procedure of line assignment which suit for assignments of weak lines. Such a procedure was created on the basis of self–consistency requirement for spectroscopic parameters. The parameters obtained from the fitting for one part of a spectrum have to predict the another part of it.

Starting from initial spectroscopic parameters we perform:

a) the calculation of energy levels, line centers, and intensities for small rotational quantum numbers J ($J = 0 \dots 3$);

b) the line assignment with check of combination differences (if possible);

c) the energy levels determination. Necessary step of the line assignment procedure is simultaneous determination of spectroscopic parameters by fitting to levels energies. This fitting procedure takes into account dark states as well as resonances between all states of resonance polyad and between states belonging to different resonance polyads. After determination of new set of spectroscopic parameters, we go to the next values of J.

It is necessary to have a source of information on the initial spectroscopic parameters which is independent of the line assignments themselves. In the case of isotopic molecules, such additional information can be obtained from data on the main isotopomer using rules valid for isotopic substitutions.[19,20]

This assignment procedure allows us to treat spectra which are caused by transitions to very high vibrational states, up to 17000 cm^{-1}.

$H_2{}^{16}O$, $H_2{}^{18}O$
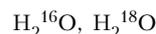
Energy structure of the second hexade and the first decade of $H_2{}^{16}O$ and $H_2{}^{18}O$ has been investigated using the intracavity laser spectrometers in the 8000–11000 cm^{-1} spectral region. Spectra were recorded at temperatures up to 1000 K. Analysis of the first and the second decades of $H_2{}^{16}O$ and $H_2{}^{18}O$ was performed in cooperation with J.M. Flaud et al. using data obtained with a Fourier transform spectrometer.[21,22]

In order to solve the inverse problem for the first decade, it is necessary to take into account the states (060), (041), and (140), which correspond to a high degree of excitation of bending vibration of a large amplitude. It is well known[23,24] that calculation of the vibrational–rotational levels of these states requires special procedures, since the matrix elements of the effective Hamiltonian, which is given in the form of the conventional power series, diverge even for small quantum numbers K_a. As a consequence, we use the Pade–Borel method of approximants[25] to calculate the energy levels. In the calculation of centers of the bands E_v, the inverse vibrational problem was solved.

Solution of the inverse problem for the first decade of the interacting states taking into account all possible resonance interactions as well as their combinations (the energy levels up to $J = 5$ were used) showed the presence of a strong perturbation of energy levels of the state (220) with $K_a = 1$.

Consideration of the resonance between the vibrational states (220) of the first decade and (070) which belong to the second decade makes it possible to explain completely the observed anomalies in the energy spectrum.[26] The standard deviation is 0.014 cm^{-1}, the maximum deviation is 0.06 cm^{-1} for all the levels involved in the fit.

It was found that the resonance between the states (220) and (070) was determined by a nondiagonal matrix element of the inverse moment of inertia of the type

$$F_k^{v_2 v_2} = <V_2 \mid b_{zz}(\Theta) \mid V_2'> \mid C\alpha^{v_2 + v_2} \ . \qquad (3)$$

Here C is a constant, $\alpha = 12$, and F_k is the resonance constant. Formula (3) was derived by solving a model problem for the bending vibration of H_2O with the Poschl––Teller potential. As is seen from Eq. (3), F_k increases rapidly as the vibrational quantum numbers of the bending vibration increase. Here, as a result of the proximity of the levels, the resonance corrections to the energy can become considerable already at the resonance constant $F_k = 1$, what explains the observed perturbations.

The diagram of the vibrational energy levels of H_2O is given in Fig. 5 from which it follows that a number of highly excited (with respect to V_2) vibrational levels turn out to be close in energy to the states of the lower resonance polyads, the resonances also being of a local character. The analysis of the states of the second hexade $2\upsilon + \delta$ shows that the perturbations produced, as in our case, by the interaction of the states (012) and (060) are observed in the energy spectrum.
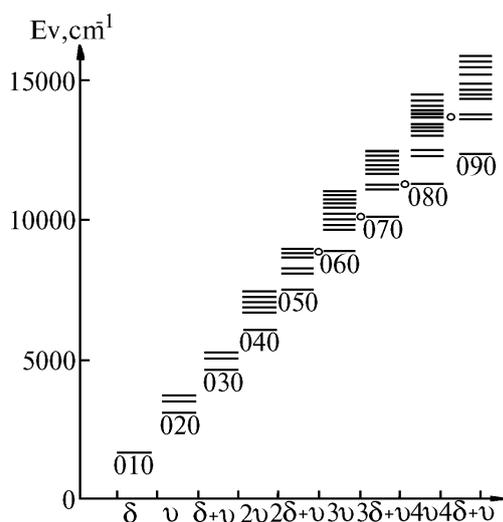

FIG. 5. Diagram of the vibrational states of the H_2O molecule. Open circles denote highly excited local resonances.

Our analysis of the energy structure of the upper polyads 4υ and $4\upsilon + \delta$ also indicates the possibility of resonance interactions of a new type. Thus, the new accidental resonance has a systematic character. Beginning with a certain vibrational energy it couples all the resonance polyads and should be taken into account when analyzing the absorption spectra and energy structure of highly excited vibrational–rotational states of water vapor molecule.

Local resonance found for the highly excited vibrational states is associated with a strong centrifugal effect, which results in excitation of a bending vibration of large amplitude. This happens because of large values of the matrix elements of the inverse moment of inertia. In this sense, new resonance differs qualitatively from the

accidental Coriolis, Darling–Dennison, and Fermi resonances considered earlier and associated with the anharmonic and Coriolis constants. New resonance couples the states with large difference of vibrational quantum numbers.

In the case of accounting for the new accidental resonance, the scheme of the construction of the resonance polyads for the water vapor molecule becomes inapplicable. The highly excited vibrational states are effectively mixed together as a consequence of the strong centrifugal effect, forming the overall reservoir of vibrational states which determines the physical and chemical properties of the molecule.

With the account for peculiarities of this resonance, namely, its local character and its existence only for highly excited states, it can be called HEL (highly excited local) resonance.

Similar resonance interactions associated with a strong centrifugal effect are likely to be between the highly excited states in isotope–substituted molecules of $H_2^{17}O$, H_2^8O, HDO, $H_2^{18}O$, or in water–like molecules H_2S, H_2Se, etc., which possess a vibration of large amplitude.

<div align="center">D₂O</div>

D_2O

The spectrum of D_2O was investigated using intracavity laser spectrometer at a pressure of 16 Torr. The $v_2 + 3v_3$ ($v_0 = 9376.05$ cm^{-1}) and $v_1 + v_2 + 2v_3$ ($v_0 = 9205.86$ cm^{-1}) bands have been recorded and analyzed for the first time.[27]

Analysis of the D_2O Fourier transform spectrum which has been recorded by P.S. Ormsby et al.[28] with an absorption path length of 240 m has led to the assignment of the bands $3v_2 + v_3$, $v_1 + v_2 + v_3$, $v_1 + 3v_2$, $2v_1 + v_2$, and $v_2 + 2v_3$ in the 6000–7000 cm^{-1} region. This has allowed determination of a large experimental set of rotational levels belonging the second hexade of interacting states of $D_2^{16}O$.

Vibrational energies and both rotational and coupling constants for the states (031), (111), (130), (210), (012), (112), and (013) of the D_2O molecule have been determined.

The fitting procedure involved 92 constants for 647 energy levels and the agreement between observed and calculated values can be seen from the statistical analysis ($\delta = |E_{calc} - E_{obs}|$):

$0.000 < \delta \le 0.003$ cm^{-1}	56.5 % of the levels
$0.003 < \delta \le 0.005$	18.6 %
$0.005 < \delta \le 0.008$	15.2 %
$0.008 < \delta \le 0.020$	9.7 %

The mean error (one standard deviation) is 0.0053 cm^{-1}. This analysis shows that the agreement is quite satisfactory considering the existence of dark states which influence the energy levels, but are not observable due to weak band intensities.

There are several examples of strong triple resonances in D_2O spectrum, for example, in the [9 4 5] (031) state the mixing coefficients for the (031), (111), and (130) states are 0.42, 0.21, and 0.35, respectively. In such cases the labeling of states is a matter of convention. Lines involving the (130) levels with $K_a = 5$ and $J = 7$, 8, ..., 11 appear only due to strong mixing, borrowing their intensity from the lines of the strong $3v_2 + v_3$ band.

HDO

The absorption spectra of a mixture of $H_2^{16}O$, $HD^{16}O$, and $D_2^{16}O$ at different concentration of deuterium have been recorded using a set of ICL spectrometers in 0.9–1.25 μm region.[29,30] The measurements were performed at different temperatures up to 1000 K.

From 667 lines recorded in the 0.9 μm spectral region, 317 lines have been assigned as transitions from ground to (003) vibrational state. We have revealed 97 energy levels of (003) vibrational state up to $J = 14$ and $K_a = 7$ (Ref. 30).

The measurements of HDO spectrum in 16 700–17 000 cm^{-1} at room temperature were made by V. Kapitanov et al. with an opto–acoustic laser spectrometer. The line centers of HDO were measured relative to known centers of H_2O with accuracy about 0.001 cm^{-1}.

Eighty six energy levels have been determined for (005) vibrational states up to $J = 11$ and $K_a = 7$. It follows from the relative line strength comparison that $5\nu_3$ band is of the "a" type with an intensity of a "b" type transition 10 times weaker.

The Watson–type rotational Hamiltonian was used to fit the spectroscopic constants of (005) vibrational state. It was found that calculation reproduces the experimental values of (005) state quite well, so the standard deviation is 0.006 cm^{-1} (Ref. 30).

A statistical analysis of 86 values of $\delta = |E_{obs} - E_{calc}|$ of the (005) vibrational states yield the following results:

$0.000 < \delta \le 0.005$ 72 % of the levels
$0.005 < \delta \le 0.010$ 19 %
$0.010 < \delta \le 0.018$ 9 %

Let us note that errors of calculation are not greater than 0.01 cm^{-1} for 91% of the levels.

The vibrational states (003) and (005) of the HDO molecule have been investigated for the first time. They are the highest excited states among (already studied) known from literature. The energy level calculations for these states appear to be reliable without taking into account any accidental resonances. This is quite opposite to the usual practice of highly excited energy levels calculations for light asymmetric top molecules (such as H_2O) when it is necessary to include a large number of intricate resonance couplings.[26,31]

The vibrational states $(00\nu_3)$ of HDO may be considered as isolated ones because the resonances of Darling–Dennison or Coriolis types are not significant due to the large difference between ν_1, $2\nu_2$, and ν_3 vibrations. The resonances between considered vibrational states and others, lying closely, are negligible for the reasons of large differences in vibrational quantum numbers.

We concluded that the energy spectrum of $HD^{16}O$ molecule should be divided into two spectra, the first includes non–resonant vibrational states of the $(01\nu_3)$ and $(00\nu_3)$ type, and the second involves the rest vibrational states. For the latter the resonance coupling is very significant, the new resonances appear at vibrational excitation growth. Vibrational states of water vapor isotopes investigated at IAO are presented in Fig. 6.
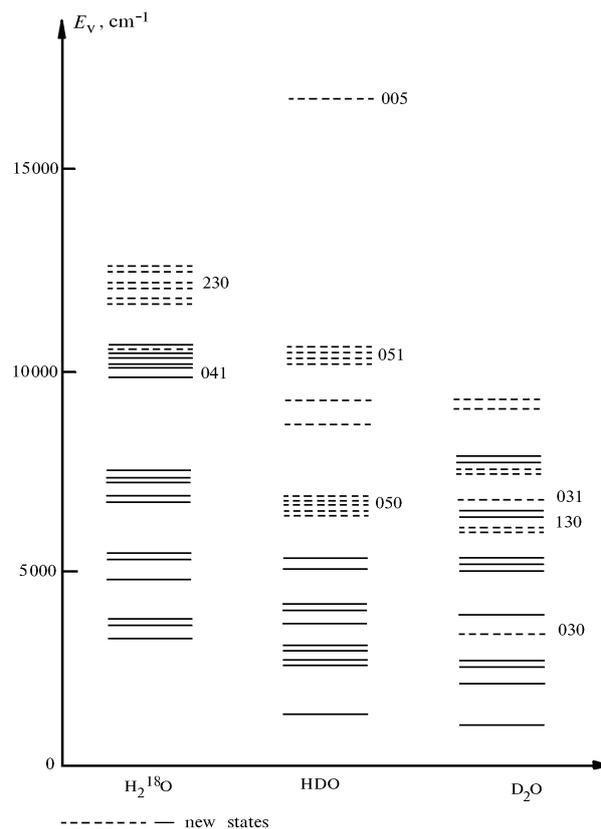
FIG. 6. *Vibrational states of water molecule isotopomers (dashed lines denote the bands investigated at IAO).*

Table V summarizes data obtained for energy structure of water vapor isotopes.

TABLE V. *The vibrational–rotational bands of the water isotopomers investigated at the IAO SB RAS.*

Spectral region, cm^{-1}	Band	Experiment	Theoretical analysis				Refs.
$H_2^{16}O$							
8100–9500		ICL**					6, 11,13, 32
	111–000		a	b	c	d	
	012–000		a	b	c		
	210–000		a		c		
	031–000		a		c	d	
	130–000		a	b	c	d	
	060–000					d	
	041–010		a				
	121–010		a			d	
10200–11000		ICL					26,33
	003–000		a				
	201–000		a		c		
	121–000		a		c	d	
	041–000		a				
	102–000		a				
	300–000		a				
	022–000		a			d	
	220–000		a			d	
	070–000*		a			d	
	211–000*						

TABLE V (continued).

Spectral region, cm⁻¹	Band	Experiment	Theoretical analysis			Refs.
11255–12160		FTS				22, 37
	131–000*		a			
	230–000*		a			
	310–000*		a			
	211–000*		a			
	112–000*		a			
	013–000*		a			
16758–17030		OA				36
	401–000		a	b	c	
	321–000		a	b		
	302–000		a			
	222–000		a			
HD¹⁶O						
6000–7000		FTS				35
	101–000		a			
	210–000		a		d	
	050–000		a		d	
	021–000		a			
	130–000		a			
8558–9150		ICL				29
	012–000 *		a			
9160–9390		ICL				27
	310–000*		a			
	121–000*		a			
10280–10700		ICL				30
	211–000*		a		d	
	051–000*		a		d	
	003–000*		a			
	131–000*		a			
	400–000*		a			
16746–17012		OA				30
	005–000 *		a			
D₂¹⁶O						
6000–7000		FTS				28
	012–000*		a			
	111–000		a			
	130–000*		a			
	210–000*		a			
	031–000*		a			
	121–000*		a			
9100–9500		ICL				27
	112–000 *					
	113–000 *					
9100–9500		ICL				27
	031–000 *		a			
	111–000 *		a			
9500–11250		FTS				21
	003–000		a			
	121–000		a		d	
	102–000		a			
	022–000		a		d	
9500–11250		FTS				21
	070–000*		a		d	
	201–000		a			
	041–000		a			
	300–000		a			
	200–000*		a		d	
11305–13609						22, 37
	131–000*		a			
	230–000*		a			
	310–000*		a			
	211–000*		a			
	112–000*		a			
	013–000*		a			

* − new bands, ** − type of spectrometer,

ICL − intracavity laser spectrometer, OA − opto−acoustic spectrometer, FTS − Fourier transform spectrometer, a − the line assignment, energy level and spectroscopic constant determination, b − the dipole moment parameters determination, c − the line shift and half−width coefficients calculations, and d − the upper state is involved in the HEL resonance.

2.3. H₂S energy level structure

The absorption spectra of H_2S within the range from 2000 to 11 147 cm⁻¹ have been obtained with the spectral resolution of 0.006 ... 0.021 cm⁻¹ using Fourier transform spectrometer at Kitt Peak National observatory.[38]

The transitions of 20 bands have been assigned for the first time and 8 others re−analyzed so that accurate energy levels, band origins, rotational parameters, and the effective vibrational Hamiltonian constants could be determined to calculate the highly excited vibrational levels (Table VI). Comparison of calculated and measured H_2S spectrum is presented in Fig. 7.
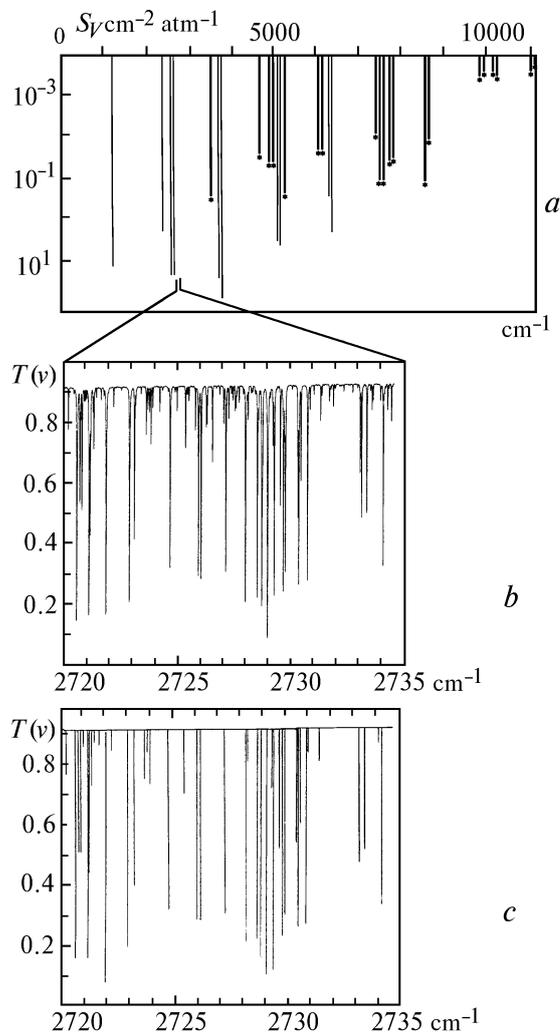

FIG. 7. Rotational−vibrational bands of H_2S molecule (∗ − new bands) (a); experimental (b) and calculated (c) region of spectra.

TABLE VI. *Upper vibrational state energy levels of* $H_2{}^{32}S$ (cm^{-1}).

$V_1V_2V_3$	E_{calc}	E_{obs}	o.—c.	Kozin (Ref. 40) MORBID	Senekowisch (Ref. 39) *ab initio*
010	1182.561	1182.5742	0.014	1182.44	1190.4
020	2352.950	2353.9644	0.014	2353.83	2372.0
100	2614.355	2514.4080	0.052	2614.66	2531.0
001	2628.431	2628.4551	0.024	2628.56	2631.0
030 *	3513.789	3513.7900	0.001	3513.17	3543.5
110	3779.1665	3779.1665	− 0.012	3779.29	3794.6
011	3789.273	3789.2690	0.004	3789.66	3799.8
040 *	4661.699	4661.6992	0.000	4659.48	4703.7
120 *	4932.715	4932.6992	− 0.016	4932.91	4960.1
021 *	4939.122	4939.1045	− 0.017	4939.82	4960.0
200	5145.014	5144.9862	− 0.028	5145.52	5154.2
101	5147.256	5147.2207	− 0.036	5147.12	5155.5
002 *	5243.055	5243.1016	0.046	5243.38	5251.2
130 *	6074.585	6074.5825	− 0.003	6074.50	6115.6
031 *	6077.597	6077.5952	− 0.002	6078.05	6110.2
210	6288.160	6288.1465	− 0.013	6288.37	6307.7
111	6289.220	6289.1733	− 0.047	6288.99	6307.8
121 *	7420.074	7420.0908	0.017	7419.92	7452.1
102 *	7576.395	7576.3813	− 0.014	7576.45	7589.4
201 *	7576.555	7576.5439	− 0.011	7576.42	7589.4
300 *	7752.288	7752.2646	− 0.023	7752.40	7768.4
003 *	7779.341	7779.3184	− 0.023	7779.60	7789.3
112 *	8697.070	8697.1426	0.072	8696.58	8723.0
211 *	8697.115	8697.1553	0.040	8696.48	8723.1
202 *	9911.008	9911.0225	0.015	9910.77	9848.0
301 *	9911.016	9911.0225	0.007	9910.75	9929.1

* − new bands

The results of *ab initio* calculations[39] and calculations by Kozin and Jensen[40] using variational MORBID method are presented in Table VI along with our data.

3. PRESSURE LINE SHIFTS

An increased interest in line shifts by pressure in molecular vibrational—rotational spectra has been observed in recent years. This interest is caused by spectroscopic applications to remote sensing of trace constituents in the Earth's atmosphere.[41]

3.1 Experiment

The experimental data on H_2O absorption line shifts within the high frequency region caused by N_2, O_2, and air pressure were obtained using a high resolution Nd:glass laser spectrophotometer, a diode laser spectrometer, an opto—acoustic laser spectrometer, and in collaboration with B.E. Grossmann and E.V. Browell using a spectrophotometer with a ring dye laser,[42] and with W. Lafferty using a Fourier transform spectrometer.[43] The spectral line widths of the lasers were about two order of magnitude less than the Doppler width of the investigated absorption lines, that enabled us to neglect the effect of the instrumental function of the spectrophotometers on the measured values.

Use of dual—channel experimental scheme is a characteristic feature of our measurements: two White cells are used in the laser spectrophotometers at a different pressure of the gas mixture in each of them. One of the cell contains pure water vapor at a pressure about 1 Torr, and the other cell contains gas mixture at a pressure of 100—760 Torr. Simultaneous measurements of the absorption in each cell provides highly accurate measurements (− 0.001 cm^{-1}) of the line shifts.

3.2. Line shift calculations

First calculations of water vapor line shift coefficients were done by Davies and Oli[42] for the ν_2 band. An agreement with experimental values of Eng et al.[45–46] was found to be poor both for the case of Anderson—Tsao—Curnutte (ATC) theory and for the quantum Fourier transform (QFT) method calculations.

Later Bosenberg[47] has found the drastic disagreement between the measured values for lines of $3\nu_1 + \nu_3$ band and those calculated for pure rotational lines. The calculated data differ from experimental ones by order of magnitude or by sign. The detailed analysis of the data carried out in our previous works[42,48,49] shows that the "simple" ATC method can be used for the line shift of the vibrational—rotational H_2O bands. The method was shown to be valid if the intramolecular interactions and the contribution of the isotropic part of the polarization potential are taken into account more accurately. A modification of the ATC method required for correct calculation of the line shift coefficients is described in Refs. 42 and 48–53.

In the ATC method the spectral line half—width γ_{if} and line center shift δ_{if} for the transition $i \to f$, where i and f are sets of quantum numbers of the initial and the final states, are given by the following formula[54,55]:

$$\gamma_{if} - i\delta_{if} = \frac{n}{c} \sum_j \rho(j) \int_0^\infty d\upsilon \, \upsilon \, F(\upsilon) \times$$

$$\times \left(\sum_{b_c(j)}^\infty d\,b\,b\,S_{if}(j, b, \upsilon) + \frac{b_c^2(j)}{2} \right), \tag{4}$$

where n is the concentration of buffer gas molecules, c is the speed of light, $\rho(j)$ is the population of the level j of buffer gas molecules, υ is relative velocity of colliding molecules; $F(\upsilon)$ is the Maxwellian distribution function, and b is the impact parameter. The complex interruption function $S_{if}(j, b, \upsilon)$ determines the contribution of the collision (j, b, and υ characterize the type of collision) to broadening and shifting, the interruption function in the ATC method is represented as a sum of the first— and second—order terms of the expansion of the intermolecular potential

$$S_{if}(j, b, \upsilon) = S_{if}^{(1)}(j, b, \upsilon) + S_{if}^{(2)}(j, b, \upsilon) . \tag{5}$$

Real part of the interruption function determines the half—width, and the imaginary part determines the line shift. Correspondingly, line shift also can be represented as

$$\delta = \delta_{if}^{(1)} + \delta_{if}^{(2)} . \tag{6}$$

Vibrational excitation leads to the growth of the contribution of the isotropic term of the polarization potential to the line shift which strongly depends on the

variations of the H_2O molecule polarizability, which, in its turn, determines the value of the dispersion constant C_6 in the intermolecular potential.

　　If the broadening is due to N_2 and O_2, and the dipole–quadrupole, induction, and dispersion terms of the intermolecular forces are taken into account, then the interruption function (5) is presented as follows:

$$S_{if}^{(1)}(j,\,b,\,\upsilon) = -\,i\,\frac{3\pi}{8\,h\upsilon\,b^5}\,<V_j|\alpha_2|V_j> \times$$

$$\times \left\{\, [\ <V_i|\mu^2|V_i> - <V_f|\mu^2|V_f>\ ] \,+\right.$$

$$\left.+\ \frac{3\,\varepsilon\,\varepsilon_2}{2(\varepsilon + \varepsilon_2)}\,[\ <V_i|\alpha|V_i> - <V_f|\alpha|V_f>\ ]\,\right\};\qquad (7)$$

$$S_{if}^{(2)}(j,\,b,\,\upsilon) = \frac{4}{45\,h^2\upsilon^2\,b^6}\sum_{j'}Q(jj'|2)\times$$

$$\times\left\{\sum_{i'}D(ii'|1)\varphi_{12}(k_{ii'jj'}) + \sum_{f'}D(ff'|1)\varphi_{12}^*(k_{ff'jj'})\right\}.\qquad (8)$$

　　In Eqs. (7) and (8) α, μ, and ε are the polarizability, dipole moment, and ionization potential of the H_2O molecule, respectively; α_2 and ε_2 are the polarizability and ionization potential of the perturbing molecules. The quantities $D(ii'|1)$ and $D(ff'|1)$ are the squares of the reduced matrix elements of the H_2O dipole moment divided by $2J_i \pm 1$ (or $2J_i + 1$). Similarly, $Q(jj'|2)$ is the square of the reduced matrix element of the nuclear quadrupole moment of the perturbing molecules divided by $(2J_2 + 1)$.

　　When calculating the line center shift, the difference in the molecular parameters of the initial and the final vibrational states must be taken into account (the polarizability $<V_f|\alpha|V_f>$, the dipole moment $<V_f|\mu^2|V_f>$, the line strength of the rotational transition $D(ff'|1)$, and the frequency $\omega_{ff'}$).

　　For absorption lines of the pure rotational spectrum $V_i = V_f$, the contribution of the function $S_{if}^{(1)}(j,\,b,\,\upsilon)$ is negligible, and the line shift is determined only by the imaginary part of $S_{if}^{(1)}(j,\,b,\,\upsilon)$. The vibrational excitation contributes to both the first and the second terms of Eq. (5), and the variation of the isotropic part of the dispersion interaction is responsible for the negative sign of the line shift in the near IR and visible spectral ranges.[49] The function $S_{if}^{(1)}(j,\,b,\,\upsilon)$ contributes to a growth of the shift when the difference $<V_i|\alpha|V_i> - <V_f|\alpha|V_f>$ on the right–hand side of Eq. (7) increases, and this growth also influences the behavior of the temperature dependence of the shift.[53] Variations of the dipole moment and rotational and centrifugal constants of the H_2O molecule during the vibrational excitation are very important in calculating the H_2O line shifts.

　　Contributions coming from different types of interaction to the line shift for the ν_2 and $3\nu_1 + \nu_3$ bands of H_2O are given in Table VII.

TABLE VII. The contributions to the line shift coefficients for ν_2 and $3\nu_1 + \nu_3$ bands of H_2O (in $10^{-3}\,cm^{-1}/atm$).

f	i	$\delta_{if}^{(2)}/dq\ qq$	$\delta_{if}^{(1)}$	δ_{if}	Exp.
$3\nu_1 + \nu_3$ band (Exp., Ref. 56)					
422	523	1.15	—	−11.0	−9.9	−9.4
515	616	−2.00	0.008	−14.8	−16.9	−19.4
505	606	−2.43	—	−14.5	−16.9	−15.7
413	514	−3.55	0.022	−10.6	−14.1	−15.5
762	761	2.05	—	−25.9	−23.8	−26.1
330	431	3.34	0.030	−13.7	−10.4	−10.3
331	432	3.45	—	−14.5	−11.1	−12.0
660	661	1.95	0.014	−28.1	−26.1	−26.3
321	422	0.64	0.003	−10.8	−10.2	−10.6
			0.013			
			—			
			0.023			
			0.006			
			0.003			
ν_2 band (Exp., Ref. 57)					
634	743	−5.11	—	−0.78	−5.95	−5.4
141	523	−2.18	0.057	−0.52	−2.73	−2.2
817	928	−8.52	—	−1.35	−9.91	−9.1
431	524	8.37	0.018	−0.70	7.77	7.2
321	414	4.38	—	−0.54	3.91	2.9
141	321	−2.81	0.034	−0.53	−3.39	−2.1
211	202	7.02	0.100	−0.46	6.65	5.0
422	413	7.00	0.067	−0.53	6.51	5.4
634	541	−5.54	—	−0.91	−6.55	−3.8
734	725	5.61	0.051	−0.58	5.05	4.9
533	524	6.28	0.095	0.76	5.56	4.0
			0.037			
			—			
			0.104			
			0.021			
			0.038			

　　In the line shift calculation the only fitting parameter, polarizability of the upper state, is used. The polarizability of the H_2O molecule in the excited vibrational state is determined by the fitting of the calculated value of the line shift to the measured for one or several lines. The line shifts of the band caused by the pressure of foreign gases as well as the shift of other lines of the band are calculated using the value of the polarizability sought.

　　The analysis of line shift coefficients using ATC method has been performed for ν_2, ν_1, ν_3, $\nu_1 + \nu_2 + \nu_3$, $\nu_2 + 2\nu_3$, $2\nu_1$, $\nu_1 + \nu_3$, $2\nu_3$, $2\nu_2 + \nu_3$, $\nu_2 + \nu_3$, $\nu_1 + \nu_2$, $2\nu_1 + \nu_3$, $3\nu_1 + \nu_3$, $2\nu_1 + 2\nu_2 + \nu_3$, $\nu_1 + 3\nu_3$, and $4\nu_1 + \nu_3$ bands of H_2O. The overall agreement is satisfactory, that is seen from the following statistical analysis:

$\Delta \le 0.0015$	63.9 % of all lines
$0.0015 < \Delta \le 0.0030$	30.6 %
$0.0030 < \Delta \le 0.0045$	2.8 %
$0.0045 < \Delta$	2.8 %

were $\Delta = |\delta_{calc} - \delta_{exp}|$ $(cm^{-1}\cdot atm^{-1})$.

CONCLUSION

The above discussed results of the investigations into the absorption spectra of atmospheric and contaminating gases are of great importance in some traditional applications. On the one hand, the spectroscopic data obtained for the parameters of highly excited vibrational–rotational states of molecules form the information base for solving the inverse problems on determination of the intra– and intermolecular potentials, parameters of the dipole moment, and so on. On the other hand, the results of such spectroscopic studies constitute the spectroscopic data bank in the high–frequency range, including the line centers, intensity, and coefficients of line broadening and shift by pressure. Combination of the precise spectroscopic information is a reliable basis for developing optical models of the molecular atmosphere both for sources of nonselective broad–band optical radiation and for different lasers.

REFERENCES

1. V.E. Zuev, *Laser Beams in the Atmosphere* (Consultants Bureau, Plenum Publishing Corporation, New York, 1982).
2. V.E. Zuev, V.P. Lopasov, and M.M.Makagon, Appl.Optics **10**, No. 10, 1015—1020 (1971).
3. V.P. Kochanov, L.N. Sinitsa, A.M. Solodov, et al., Opt. Communs. **51**, 409 (1984).
4. J.U. White, J. Opt. Soc. Am. **32**, 285 (1942).
5. S.M. Chernin and E.G. Barskaya, Atm. Opt. **2**, No. 12, 1124—1136 (1989).
6. A.D. Bykov, Yu.N. Ponomarev, and L.N. Sinitsa, Opt. Atm. **1**, No. 2, 3 (1988).
7. B.V. Bondarev, V.A. Kapitanov, S.M. Kobtsev, and Yu.N.Ponomarev, Opt. Atm. **1**, No. 10, 18 (1988).
8. L.A. Pakhomycheva, E.A. Sviridenkov, A.F. Suchkov, L.V. Titova, and S.S. Churilov, Zh. Eksp. Teor. Fiz. Pis'ma Red. **12**, 60 (1970); [Sov. JETP Letters **12**, 43 (1970)].
9. S.F. Luk'yanenko, M.M. Makogon, and L.N. Sinitsa, *Intracavity Laser Spectroscopy* (Nauka, Novosibirsk, 1985), 121 pp.
10. L.N. Sinitsa, Kvant. Elektron. **4**, No. 1, 148 (1977).
11. V.P. Kochanov, V.I. Serdyukov, and L.N. Sinitsa, *Use of the F_2^-:LiF Color–Center Laser in Intracavity Laser Spectroscopy*, Optica Acta **32**, 1273 (1985).
12. L.N. Sinitsa, J. de Physique **IV**, C4—629 (1994).
13. V.E. Zuev, V.P. Lopasov, and L.N. Sinitsa, Opt. Spektrosk. **45**, No. 3, 590 (1978).
14. L.N. Sinitsa, J. Quant. Radiat. Spectrosc. Transf. **48**, 721 (1992).
15. L.N. Sinitsa, J. Mol. Spectrosc. **84**, 57 (1980).
16. V.E. Zuev, V.P. Lopasov, L.N. Sinitsa, and A.M. Solodov, J. Mol. Spectrosc. **94**, 208 (1982).
17. L.N. Sinitsa and G.A. Vandysheva, Atm. Opt. **3**, No. 4, 320—324 (1990).
18. G.A. Vandysheva, V.N. Savel'ev, and L.N. Sinitsa, Atm. Opt. **3**, No. 4, 325—328 (1990).
19. A.D. Bykov, O.N. Ulenikov, and Yu.S. Makushkin, J. Mol. Spectrosc. **85**, 462 (1981).
20. A.D. Bykov, V.S. Makarov, N.I. Moskalenko, O.V. Naumenko, O.N. Ulenikov, and O.V. Zotov, J. Mol. Spectrosc. **123**, 126 (1987).
21. A.D. Bykov, O.V. Naumenko, L.N. Sinitsa, J.—Y. Mandin, J.—P. Chevillard, C. Camy—Peyret, and J.M. Flaud, J. Mol. Spectrosc. (to be published).
22. A.D.Bykov, O.V. Naumenko, L.N. Sinitsa, T.M. Petrova, A.P. Shcherbakov, J.—Y.Mandin, J.—P.Chevillard, C. Camy—Peyret, and J.M. Flaud, J. Mol. Spectrosc. (to be published).

23. V.I. Starikov and V.G. Tyuterev, J. Mol. Spectrosc. **95**, 2887 (1982).
24. Yu.S. Makushin, O.V. Naumenko, and O.N. Ulenikov, J. Mol. Spectrosc. **103**, 221 (1984).
25. O.L. Polyanskii, J. Mol. Spectrosc. **112**, 79 (1985).
26. A.D. Bykov, O.V. Naumenko, and L.N. Sinitsa, Atm. Opt. **3**, No. 10, 1014—1018 (1990).
27. A.D. Bykov, V.P. Lopasov, Yu.S. Makushkin, L.N. Sinitsa, O.N. Ulenikov, and V.E. Zuev, J. Mol. Spectrosc. **94**, 1 (1982).
28. P.S. Ormsby, K.N. Rao, M. Winnewisser, B.P. Winnewisser, O.V. Naumenko, A.D. Bykov, and L.N. Sinitsa, J. Mol. Spectrosc. **158**, 109 (1993).
29. A.D. Bykov, Yu.S. Makushkin, V.I. Serdyukov, L.N. Sinitsa, O.N. Ulenikov, and G.A. Ushakova, J. Mol. Spectrosc. **104**, 397 (1984).
30. A.D. Bykov, V.A. Kapitanov, O.V. Naumenko, T.M. Petrova, V.I. Serdyukov, and L.N. Sinitsa, J. Mol. Spectrosc. **153**, 197 (1992).
31. V.I. Starikov and S.N. Michailenko, Atm. Opt. **4**, No. 6, 424—429 (1991).
32. V.N. Cherepanov, V.P. Kochanov, Yu.S. Makushkin, L.N. Sinitsa, A.M. Solodov, O.N. Sulakshina, and O.K. Voitsekhovskaya, J. Mol. Spectrosc. **111**, 173 (1985).
33. L.N. Sinitsa, SPIE Proc. **1811**, 58 (1978).
34. A.D. Bykov, O.V. Naumenko, T.M. Petrova, V.I. Serdyukov, L.N. Sinitsa, and E.V. Tsyganova, SPIE Proc. **2205**, 244 (1993).
35. O.V. Naumenko, A.D. Bykov, L.N. Sinitsa, B.P. Winnewisser, M. Winnewisser, P.S. Ormsby, and K.N. Rao, SPIE Proc. **2205**, 248—252.
36. A.B. Antipov, A.D. Bykov, V.A. Kapitanov, et al, J. Mol. Spectrosc. **89**, 449 (1981).
37. J.M. Flaud, C. Camy—Peyret, J.—Y. Mandin, A.D. Bykov, T.M. Petrova, L.N. Sinitsa, and A.P. Sherbakov, in: *The Future of Spectroscopy Conference*, Canada (1994), p. 134.
38. L. Brown, D. Crisp, J. Crisp, A.D. Bykov, O.V. Naumenko, and L.N. Sinitsa, SPIE Proc. **2205**, 238 (1993).
39. J. Senekovich, S. Carter, A. Zilch, H.J. Werner, and N.C. Hardy, J. Chem. Phys. **90**, 783 (1989).
40. I.N. Kozin and P. Jensen, J. Mol. Spectrosc. **161**, 186 (1993).
41. V.V. Zuev, Yu.N. Ponomarev, A.M. Solodov, B.A. Tikhomirov, and O.A. Romanovskii, Opt. Lett. **10**, 318 (1985).
42. B.E. Grossmann, E.V. Browell, A.D. Bykov, et al., Atm. Opt. **3**, No. 7, 617—630 (1990).
43. A.D. Bykov, N.N. Lavrent'eva, V.N. Savel'ev, L.N. Sinitsa, A.M. Solodov, W.J. Lafferty, and V.B. Olson, in: *Abstracts of Reports at the First All–Russian Symposium on Optics of the Atmosphere and Ocean*, Tomsk (1994), Vol. 1, p. 45.
44. R.W. Davies and B.A. Oli, J. Quant. Radiat. Spectrosc. Transf. **20**, 95 (1978).
45. R.S. Eng, P.L. Kelley, A. Mooradian, A.R. Galawa, and T.C. Harman, Chem. Phys. Lett. **19**, 524 (1973).
46. R.S. Eng, P.L. Kelley, A.R. Galawa, T.C. Harman, and K.W. Nill, Mol. Phys. **28**, 653 (1974).
47. J. Bosenberg, Appl. Opt. **24**, 531 (1985).
48. A.D. Bykov, Yu.S. Makushkin, and V.N. Stroinova, Opt. Spektrosk. **64**, No. 3, 517 (1988).
49. A.D. Bykov, E.A. Korotchenko, Yu.S. Makushkin, et al., Opt. Atm. **1**, No. 1, 40 (1988).
50. A.D. Bykov, N.N. Lavrent'eva, and L.N. Sinitsa, Atmos. Oceanic Opt. **5**, No. 9, 587—594 (1992).

51. A.D. Bykov, N.N. Lavrent'eva, and L.N. Sinitsa, Atm. Opt. **4**, No. 7, 518—523 (1991).

52. A.D. Bykov, N.N. Lavrent'eva, and L.N. Sinitsa, Atmos. Oceanic Opt. **5**, No. 11, 728—730 (1992).

53. A.D. Bykov, Yu.S. Makushkin, L.N. Sinitsa, and V.N. Stroiniva, Opt. Atm. **1**, No. 5, 31 (1988).

54. P.W. Anderson, Phys. Rev. **76**, 647 (1949).

55. C.J. Tsao and B. Curnutte, J. Quant. Radiat. Spectrosc. Transf. **2**, 41 (1962).

56. B.E. Grossman and E.V. Browel, J. Mol. Spectrosc. **138**, 562 (1989).

57. A.—M.H. Smith and S.P. Rinsland (private communication).